Appl Phys B (2010) 100: 125–130
DOI 10.1007/s00340-010-3984-z

Applied Physics B
Lasers and Optics

NO trace gas sensor based on quartz-enhanced photoacoustic spectroscopy and external cavity quantum cascade laser

V. Spagnolo · A.A. Kosterev · L. Dong · R. Lewicki · F.K. Tittel

Received: 1 March 2010 / Published online: 17 March 2010

Abstract A gas sensor based on quartz-enhanced photoacoustic detection and an external cavity quantum cascade laser was realized and characterized for trace nitric oxide monitoring using the NO R(6.5) absorption doublet at 1900.075 cm^{-1}. Signal and noise dependence on gas pressure were studied to optimize sensor performance. The NO concentration resulting in a noise-equivalent signal was found to be 15 parts per billion by volume, with 100 mW optical excitation power and a data acquisition time of 5 s.

1 Introduction

The development of compact optical sensors for nitric oxide detection is of interest for a number of applications, such as industrial emissions and process monitoring [1, 2], atmospheric chemistry [3], combustion studies [4] and medical diagnostics [5]. Nitric oxide is involved in many vital physiological processes in the human body and elevated levels of NO in exhaled human breath is correlated with airway inflammation in asthmatic patients. Furthermore, NO is also present in vehicle exhaust emissions and can produce dangerous pollutants due to complex photo-initiated reactions between NO, HCs and O_2, resulting in the production of ozone and other reactive oxygen species that cause the photochemical smog present in many major cities [6, 7]. Thus controlling the HCs and NOx vehicle emissions can have a direct impact on the effective reduction of urban photochemical smog.

Quantum cascade lasers (QCLs) are well suited for mid-infrared spectroscopic trace gas sensing due to their narrow linewidth, high power at room temperature and continuous wave (CW) operation at mid-IR wavelengths (3 to 24 μm) [8, 9]. QCLs overcome some of the drawbacks of other traditional mid-IR laser sources, i.e. the lack of continuous wavelength tunability, the large size and weight of gas lasers (e.g. CO and CO_2), the cooling requirement of lead salt diode lasers, as well as the complexity and low power of nonlinear optical sources.

Several approaches utilizing QCLs for the optical sensing of trace NO have been reported [10]. Faraday modulation spectroscopy has been demonstrated to reach a detection sensitivity of a few parts per billion by volume (ppb) [11, 12]. Spectrometers based on a QCL and absorption detection in a multipass cell can lead to NO detection limit of the order of single ppb and below [1, 2, 13]. Sub-ppb concentration levels can also be detected using Cavity Ring-down Spectroscopy [14–16]. An integrated cavity output spectroscopy (ICOS) based sensor utilizing a QCL was reported to reach a detection sensitivity of sub-ppb in 4 s [17].

In this paper we report the development and performance evaluation of an advanced quartz-enhanced photoacoustic spectroscopy (QEPAS) based NO sensor, utilizing a CW, thermoelectrically cooled, external cavity quantum cascade laser (EC-QCL) as a light source. QEPAS [18] has been used with several QCL sources and was applied to the detection of various chemical species [18–23]. The key innovation of QEPAS is to detect optically generated sound using a rugged sharply resonant piezoelectric transducer in the form

V. Spagnolo (✉)
CNR—Istituto di Fotonica e Nanotecnologie and Dipartimento Interateneo di Fisica "M. Merlin", Politecnico di Bari, Via Amendola 173, Bari, Italy
e-mail: spagnolo@fisica.uniba.it
Fax: +39-080-5442219

A.A. Kosterev · L. Dong · R. Lewicki · F.K. Tittel
Department of Electrical and Computer Engineering, Rice University, Houston TX 77251, USA

of a quartz tuning fork with a set of unique properties such as an extremely high quality factor (Q-factor) of >10,000, small size, immunity to environmental acoustic noise and a large dynamic range. All QEPAS-based sensors reported to date employ commercially available 32.8 kHz quartz tuning forks, designed for use as frequency standards in digital clock circuits. QEPAS is a suitable technology for portable gas sensors for field and industrial applications, because it has proved to be highly immune to environmental interference, and the small size of the QEPAS absorption-sensing module permits convenient integration with QCL sources.

2 Experimental details

In this work a CW water-cooled EC-QCL (Daylight Solutions model 21052-MHF) operating at $\lambda = 5.26$ µm is employed as the spectroscopic light source. At a QCL chip temperature of 16.5°C, this laser has a tuning range of 1763–1949 cm^{-1} and a specified mode hop free tuning range of 1807–1901 cm^{-1}, corresponding to 5% of its center wavelength, with output power in excess of 100 mW over this range. The maximum tuning rate via the laser controller is 38 nm/sec and the highest measured optical power is ~250 mW. Precise and continuous control of the laser wavelength can be performed by one of the two methods. The optical frequency can be scanned over ~1 cm^{-1} by applying a modulated voltage of up to 70 V peak-to-peak at 1 Hz to a piezoelectric translator attached to the diffraction grating element of the EC-QCL. For a higher modulation frequency, an internal bias tee allows external modulation of the QCL current to obtain up to 0.1 cm^{-1} peak-to-peak optical frequency modulation at up to 2 MHz [24].

The QEPAS-based gas sensor architecture is depicted in Fig. 1. To enhance the QEPAS signal, and hence increase

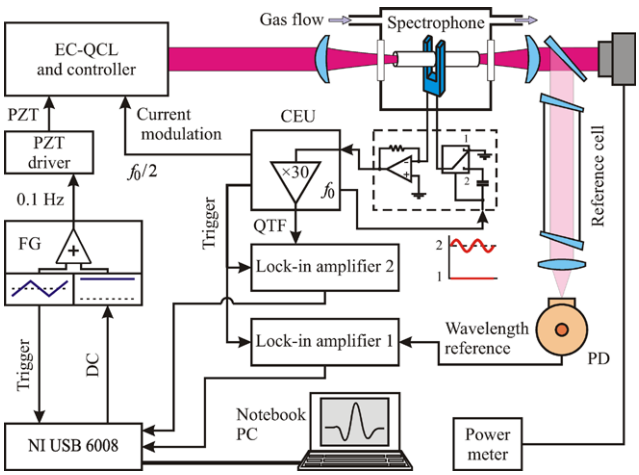

Fig. 1 Schematic of EC-QCL-based QEPAS NO sensor. PD—photodetector; FG—function generator

the trace gas detection sensitivity the quartz tuning fork (QTF) used in this work is coupled with an acoustic organ pipe type micro-resonator (MR) [25]. Metal tubes with a length of 4.0 mm each and inner diameter of 0.6 mm were mounted on both sides of the QTF. The gap between the flange of each tube and the QTF surface is ~30 µm. The Q-factor of the QTF is 17500 at 75 Torr and decreases to 3800 at atmospheric pressure, with resonant frequencies of 32406 Hz and 32398 Hz, respectively. The QEPAS spectrophone (SPh) consisting of the QTF and the MR is mounted inside a vacuum-tight cell with ZnSe windows. The pressure and flow rate of the sample gas through the SPh are controlled and maintained at the optimum level using a pressure controller (MKS Instruments Type 640) and a ball flow meter (Key Instruments). The flow of the gas mixture is set at a constant rate of 75 scc/min. The QCL beam is focused by using a 25.4 mm diameter CaF_2 lens with a 75 mm focal length and passes through the SPh tubes. Part of the laser radiation exiting the SPh is directed through an optical gas cell (reference cell, length 10 cm) filled with a 0.5% NO in N_2 and subsequently is incident on an IR detector (PD, VIGO model PDI-2TE). The second harmonic (with respect to the laser current modulation frequency) of the PD signal serves as a spectral reference.

Wavelength modulation (WM) technique is implemented by applying a sinusoidal dither to the diode laser current at half of the QTF resonance frequency and detecting the QTF response at $2f$ by means of a lock-in amplifier. The highest amplitude of the $2f$ harmonic component achieved at the absorption line center is generally lower than the highest amplitude of the $1f$ signal. However, $2f$ detection has an advantage because the residual amplitude modulation signal created at $1f$ during the laser current modulation is strongly suppressed at higher harmonics. This minimizes the background caused by the spectrally nonselective absorption of stray radiation and also minimizes the impact of distant spectral wings of interfering strong absorption lines on the measured QEPAS signal. Therefore, we perform WM by sinusoidally modulating the injection current of the laser at a frequency of $f = f_0/2 \sim 16.20$ kHz, while slowly scanning the laser wavelength using the PZT. The corresponding photoacoustic spectra are obtained by demodulating the detected signal at the frequency f_0 using a lock-in amplifier.

The piezoelectric signal generated by the QTF is detected by a custom designed transimpedance amplifier (feedback resistor $R_{fb} = 10$ MΩ). Subsequently the signal is demodulated by a lock-in amplifier (Stanford Research Model SR830) and digitalized by a USB data acquisition card (National Instruments DAQCard USB6009), which is connected to a personal computer. The control electronics unit (CEU) is used to determine the equivalent electrical parameters of the QTF: its dynamic resistance R, quality factor Q, and

resonant frequency f_0, and to pass on the 31.3 times amplified signal from the transimpedance amplifier to the lock-in amplifier. The lock-in amplifiers and a function generator (Tektronix model AFG3102) are controlled through a serial communications port (RS232) and through a USB NI card, respectively, using LabVIEW-based software. The time constant of the lock-in amplifiers was set to 30 ms for all QEPAS-based measurements reported in this work.

Many practical applications of NO detection such as exhaled breath analysis, automotive exhaust, and environmental monitoring, assume a presence of water vapor in the gas sample. Therefore, it is important to study the H_2O influence on the NO sensor performance. The V–T (vibration-to-translation) energy transfer time for NO is dependent on the presence of other molecules and intermolecular interactions. The QEPAS measurements that are performed at a detection frequency 32 kHz are more sensitive to the vibrational relaxation rate compared to the conventional PAS which is commonly performed at <4 kHz frequency. In case of slow V–T relaxation with respect to the modulation frequency ($\omega\tau_{VT} \gg 1$, where $\omega = 2\pi f$), the translational gas temperature cannot follow fast changes of the laser induced molecular vibrational excitation. Thus the generated photoacoustic wave is weaker than it would be in case of instantaneous V–T energy equilibration. Due to the high energy of the first vibrational state of NO, the V–T energy transfer is slow, e.g. in dry N_2 the relaxation time is $\tau_{VT} = 0.3$ ms and so $\omega\tau_{VT} \gg 1$ [27]. The addition of H_2O vapor enhances the V–T energy transfer rate. Water vapor is known to be an efficient catalyst for the vibrational energy transfer reactions in the gas phase. In the gas system studied in this work, H_2O is a relaxation promoter for the energy stored in slow relaxing NO vibrational states. Therefore the presence of water in the NO/N_2 gas mixture results in an increase of the detected NO QEPAS signal amplitude. Once the $\omega\tau_{VT} < 1$ condition is satisfied, the amplitude of the photoacoustic signal is not affected by changes of τ_{VT}. Therefore an increase of H_2O concentration beyond a certain level has a negligible effect on the PAS signal. Our experiments have been performed at such signal saturation conditions. QEPAS signals of comparable amplitude are observed for a dry NO/N_2 gas mixture with a NO concentration of 10 ppmv and a humidified NO/N_2 gas mixture with a NO concentration of 50 ppb. Hence, the addition of water vapor increases the QEPAS signal by more than two orders of magnitude. High concentrations of H_2O vapor are expected in many practical applications, including the analysis of exhaled breath samples and combustion products. A certified 10 ppm NO in N_2 mixture was used to obtain known concentrations of the investigated gas in the 0.05–10 ppm range. We use a Nafion material-based humidifier (PermaPure) to add water vapor to the gas mixture.

3 Results and discussion

According to the HITRAN database [26] the fundamental absorption band of NO is located in the spectral region from 1780 to 1950 cm^{-1}. In Fig. 2 a comparison between the absorption spectra measured using the reference cell and a HITRAN simulation for a gas mixture at atmospheric pressure is shown. The EC-QCL allows for access to the strong and quasi interference-free absorption doublet R(6.5) at 1900.075 cm^{-1}, which is unresolved at our pressure-temperature conditions.

To determine the influence of the modulation amplitude on the QEPAS signal we performed WM experiments by modulating the injection current of the laser by applying a sinusoidal voltage signal to the laser driver at 16.20 kHz with amplitudes in the range of 1.5 V–5 V. In Fig. 3a, the amplitude of the QEPAS signal measured for a NO concentration of 5 ppm in humidified N_2 is plotted as a function of the modulation voltage for two representative different gas mixing pressures. In the investigated range from 75 torr to atmospheric pressure the maximum QEPAS signal occurs at the maximum amplitude of 5 V. The WM signal increases when the total gas pressure decreases due to narrowing of the absorption line, while the molecular collision rate and thus the V–T relaxation rate increases with pressure. In addition, the spectrophone Q-factor increases at lower pressures. Therefore, the QEPAS signal depends on the gas pressure. The results presented in Fig. 3b depict the influence of pressure on the QEPAS signal amplitude and QTF quality factor (Q-factor) obtained for a 5 ppm NO concentration in humidified N_2. The laser modulation depth is kept fixed at its maximum value of 5 V. The optimum sensor operating con-

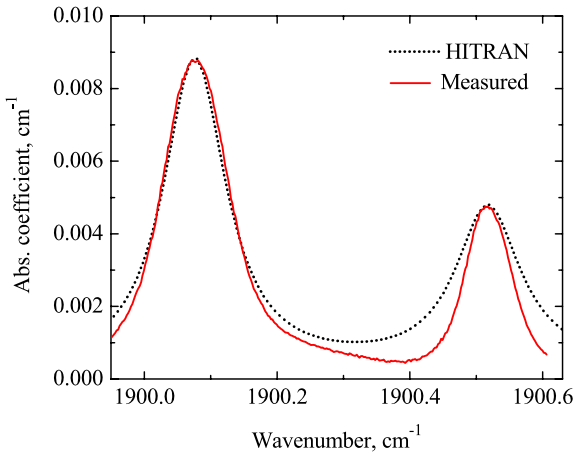

Fig. 2 Comparison between the absorption spectra measured using the reference cell (*dashed line*) and the corresponding HITRAN simulation (*solid line*) for a gas mixture of 0.5% of NO in N_2 at atmospheric pressure. The NO R(6.5) absorption doublet at 1900.075 cm^{-1} was used for the concentration measurements reported in this work

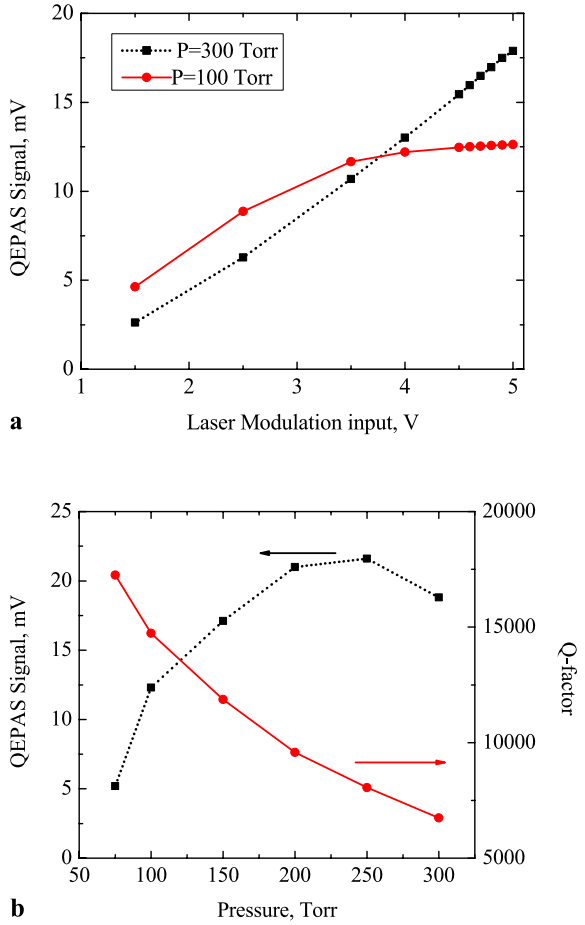

Fig. 3 (**a**) QEPAS signal amplitude measured for 5 ppm of NO in humidified N_2 plotted as a function of the QCL modulation voltage at two different pressures of the gas mixture. (**b**) QEPAS signal amplitude (*full square*) and corresponding QTF Q-factor (*full circle*) measured for 5 ppm of NO in humidified N_2 as a function of the gas mixture pressure. The laser modulation depth is kept fixed at its maximum value of 5 V

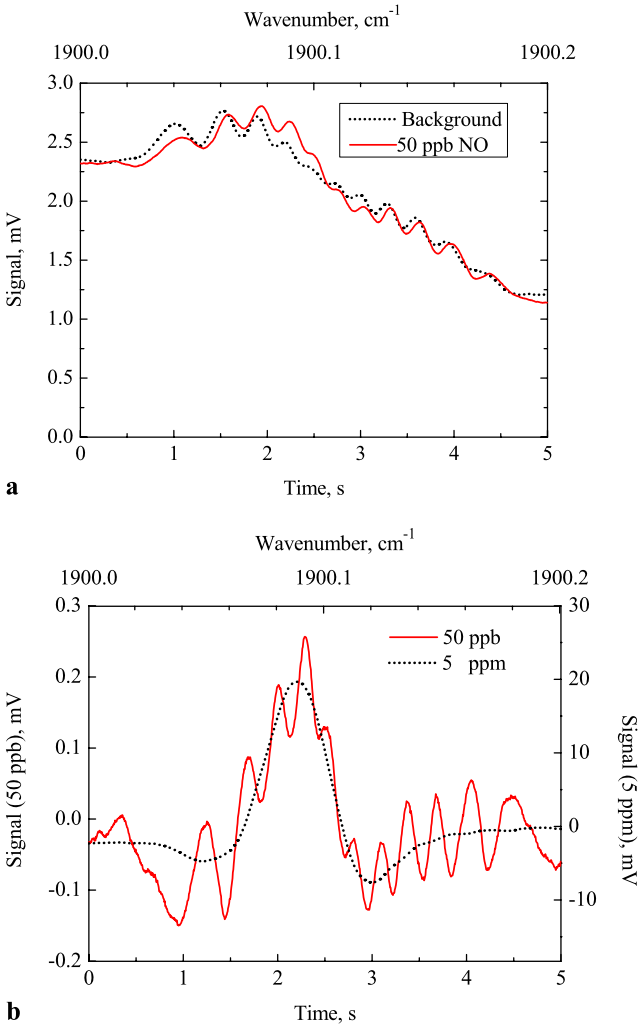

Fig. 4 (**a**) High-resolution QEPAS data acquired by co-adding 30 PZT scans, for both pure N_2 (background) and 50 ppb NO/N_2 humidified calibrated mixture. (**b**) High-resolution QEPAS data obtained after numerical subtraction of background for a 50 ppb and 5 ppm QEPAS data acquired by co-adding 30 PZT scans

ditions were found to occur at a pressure of 250 Torr and a corresponding Q-factor of 8060.

The simple optical system used in this work did not provide sufficient suppression of the stray laser light. As a result, some radiation was absorbed by the spectrophone elements and created a coherent (with respect to the laser modulation) acoustic background, which is proportional to the laser power. Therefore, the technique of locking to the absorption line peak and deriving the concentration directly from the QEPAS signal amplitude [19] was not applicable. Instead, a scanning and fitting approach is used. The time resolution of QEPAS is physically limited by the SPh Q-factor. As it is well known from classical oscillator theory, $\tau = Q/(\pi f_0)$, where τ is the time needed for the vibration amplitude to decay to $1/e$ of the initial value. In our case, $\tau = 80$ ms. In order to avoid additional resolution limitation by a lock-in amplifier while still preserving narrow bandwidth for noise reduction, its time constant was set to 30 ms with a 12 dB/oct filter slope. It was verified experimentally that such settings does not distort the observed absorption line shape for our experimental conditions.

The background signal is sufficiently stable to allow NO concentration measurements using numerical background subtraction but also carries a shifting fringe-like interference pattern, which is the primary sensitivity-limiting factor in our measurements. Figure 4(a) shows the results of co-adding QEPAS data acquired while performing 30 PZT scans, for both pure N_2 (background) and 50 ppb NO in humidified N_2 in the system. Figure 4(b) presents the results of numerical subtraction of those two curves, as well as the 5 ppm QEPAS signal acquired in the same manner. Stepwise concentration measurements are performed to verify the linearity of the QEPAS signal as a function of the NO concentration. A trace gas standard generator is used to pro-

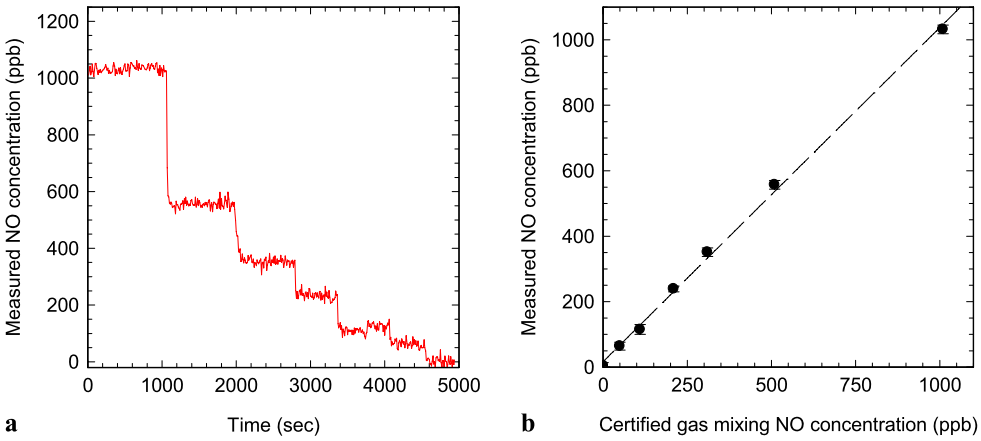

Fig. 5 (**a**) Measured NO concentrations obtained by varying settings of a commercial trace gas standard generator (Kin-Tek Model 491M). (**b**) Calibration curve obtained from measured QEPAS signals and corresponding NO concentrations using Kin-Tek gas generator

duce NO concentrations in the range 0–2 ppmv, using humidified N_2 as the diluting gas. For this purpose repetitive high-resolution scans similar to those shown in Fig. 4, each 5 s long, are performed. Spectral alignment of the scans is ensured by means of the reference gas cell and a feedback loop designed to keep the absorption peak (1900.075 cm^{-1}) detected in the reference cell at the same place on each scan. This is achieved by applying a computer-controlled DC offset to the PZT voltage (see Fig. 1). A single background measurement performed at the beginning of this experiment is used for the QEPAS data correction. After the background subtraction, the NO concentration is derived based on the general linear fit (GLF) method and the corresponding "Virtual Instrument" (VI) from the National Instruments LabView package. Namely, the experimentally acquired spectral data are represented as a linear combination of a scaled low-noise 2f QEPAS spectrum acquired at a high NO concentration and an offset. The scaling factor yields the concentration of the current NO sample.

The results are depicted in Fig. 5a. Based on the scatter of measured concentrations for each NO dilution ratio, the noise-equivalent NO concentration (1σ) is determined to be 15 ppb. Data for each step are averaged and plotted against the NO concentrations derived from the dilution ratio of the gas standard generator (Fig. 5b). The results confirm the linearity of the QEPAS sensor response to the NO concentration.

The achieved sensitivity of 15 ppb in 5 s does not represent the ultimate detection sensitivity of this sensor platform because the sensitivity limitation is due to stray radiation rather than thermal noise of the QTF. An estimate of the combined thermal QTF and transimpedance amplifier noise in the 8.33 Hz band set by the lock-in amplifier in our experiments is 0.13 mV. The experimentally measured signal is ∼20 mV for a 5 ppmv NO concentration. Thus, in ideal conditions of no stray radiation background the sensitivity is expected at the ∼30 ppb level in 100 ms (three times the lock-in amplifier time constant), or ∼10 ppb in 1 s and ∼4 ppb in 5 s. In this case, the normalized noise-equivalent absorption coefficient would be NNEA $= 3.6 \times 10^{-9}$ cm^{-1} $W/Hz^{½}$. This value is comparable to the QEPAS results obtained for fast-relaxing molecules, which confirms that the V–T relaxation of NO at 250 Torr in the presence of water vapor is sufficiently fast and complete.

4 Conclusions

The achieved detection sensitivity of 15 ppb in 5 s can be compared with other results reported in literature when detecting NO in the same spectral range. In [28] the authors used a compact ICOS cell and achieved 2 ppb in 15 s. In [29] the authors used a conventional photoacoustic spectroscopy to detect NO in dry N_2. They reported a 500 ppb sensitivity with a 10 s integration time constant (equivalent to ∼20–30 s time resolution), using a laser with 8 mW optical power, and an estimated NNEA $= 1.1 \times 10^{-7}$ cm^{-1} $W/Hz^{½}$. Thus, the QEPAS technology is competitive in terms of sensitivity, at the same time providing a more compact sensor design and smaller sample volume. The next step will be the implementation of a low-loss mid-infrared single mode fiber system to couple the QCL source with the spectrophone. Fiber optics will make it possible to convert our reported sensor into a portable device suitable for field applications. Furthermore, it will also help to suppress the background, which can potentially increase the NO detection sensitivity about three times.

Acknowledgements The authors acknowledge helpful discussions with Sam Crivello and Michael Pusharsky of Daylight Solutions. V. Spagnolo acknowledges financial support from both the Regione Puglia "Intervento Cod. DM01, Progetti di ricerca industriale connessi con la strategia realizzativa elaborata dal Distretto Tecnologico della Meccatronica" and the II. Faculty of Engineering of the Politecnico di Bari. The Rice University group acknowledges the financial support from a National Science Foundation Engineering Research Center sub award for "Mid-infrared technologies for health and the Environment (MIRTHE)" from Princeton University, and grant C-0586 from The Welch Foundation.

References

1. D.D. Nelson, J.H. Shorter, J.B. McManus, M.S. Zahniser, Appl. Phys. B **75**, 343 (2002)
2. G. Wysocki, A.A. Kosterev, F.K. Tittel, Appl. Phys. B **80**, 617 (2005)
3. J.H. Steinfeld, S.N. Pandis, *Atmospheric Chemistry and Physics: from Air Pollution to Climate Change* (Wiley, New York, 1998)
4. H. Gupta, L.S. Fan, Ind. Eng. Chem. Res. **42**, 2536 (2003)
5. J.H. Shorter, D.D. Nelson, J.B. McManus, M.S. Zahniser, D.K. Milton, IEEE Sens. J. **10**, 76 (2010)
6. W.T. Piver, Environ. Health Perspect. **96**, 131 (1991)
7. W.T. Luke, P. Kelley, B.L. Lefer, J. Flynn, B. Rappenglu, M. Leuchner, J.E. Dibb, L.D. Ziemba, C.H. Anderson, M. Buhr, Atmos. Environ. (2010). doi:10.1016/j.atmosenv.2009.08.014
8. M. Troccoli, L. Diehl, D.P. Bour, S.W. Corzine, N. Yu, C.W. Wang, M.A. Belkin, G. Höfler, R. Lewicki, G. Wysocki, F.K. Tittel, F. Capasso, J. Lightw. Technol **26**, 3534 (2008)
9. R.F. Curl, F. Capasso, C. Gmachl, A.A. Kosterev, B. McManus, R. Lewicki, M. Pusharsky, G. Wysocki, F.K. Tittel, Chem. Phys. Lett. **487**, 1 (2010)
10. C. Di Franco, A. Elia, V. Spagnolo, G. Scamarcio, P.M. Lugarà, E. Ieva, N. Cioffi, L. Torsi, G. Bruno, M. Losurdo, M.A. Garcia, S.D. Wolter, A. Brown, M. Ricco, Sensors **9**, 3337 (2009)
11. H. Ganser, W. Urban, J.M. Brown, Mol. Phys. **101**, 545 (2003)
12. R. Lewicki, J.H. Doty, R.F. Curl, F.K. Tittel, G. Wysocki, Proc. Natl. Acad. Sci. USA **106**, 12587 (2009)
13. J.B. McManus, J.H. Shorter, D.D. Nelson, M.S. Zahniser, D.E. Glenn, R.M. McGovern, Appl. Phys. B **92**, 387 (2008)
14. B.A. Paldus, C.C. Harb, T.G. Spence, R.N. Zare, C. Gmachl, F. Capasso, D.L. Sivco, J.N. Baillargeon, A.L. Hutchinson, A.Y. Cho, Opt. Lett. **25**, 666 (2000)
15. A.A. Kosterev, A.L. Malinovsky, F.K. Tittel, C. Gmachl, F. Capasso, D.L. Sivco, J.N. Baillargeon, A.L. Hutchinson, A.Y. Cho, Appl. Opt. **40**, 5522 (2001)
16. T. Nakayama, T. Ide, F. Taketani, M. Kawai, K. Takahashi, Y. Matsumi, Atmos. Environ. **42**, 1995 (2008)
17. M.L. Silva, D.M. Sonnenfroh, D.I. Rosen, M.G. Allen, A. O'Keefe, Appl. Phys. B **81**, 705 (2005)
18. A.A. Kosterev, Yu.A. Bakhirkin, R.F. Curl, F.K. Tittel, Opt. Lett. **27**, 1902 (2002)
19. A.A. Kosterev, F.K. Tittel, D. Serebryakov, A. Malinovsky, A. Morozov, Rev. Sci. Instrum. **76**, 043105 (2005)
20. M.D. Wojcik, M.C. Phillips, B.D. Cannon, M.S. Taubman, Appl. Phys. B **85**, 307 (2006)
21. R. Lewicki, G. Wysocki, A.A. Kosterev, F.K. Tittel, Opt. Exp. **15**, 7357 (2007)
22. A.A. Kosterev, G. Wysocki, Y. Bakhirkin, S. So, R. Lewicki, M. Fraser, F.K. Tittel, R.F. Curl, Appl. Phys. B **90**, 165 (2008)
23. A. Elia, P.M. Lugarà, C. Di Franco, V. Spagnolo, Sensors **9**, 9616 (2009)
24. G. Hancock, J.H. van Helden, R. Peverall, G.A.D. Ritchie, R.J. Walker, Appl. Phys. Lett. **94**, 201110 (2009)
25. S. Schilt, A.A. Kosterev, F.K. Tittel, Appl. Phys. B **95**, 813 (2009)
26. Available online: http://www.hitran.com
27. R. Sarmiento, I.E. Santosa, S.T. Persijn, L.J.J. Laarhoven, F.J.M. Harren, in *Proceedings Forum Acusticum 2005*, p. L139, Budapest (2005)
28. Y.A. Bakhirkin, A.A. Kosterev, C. Roller, R.F. Curl, F.K. Tittel, Appl. Opt. **43**, 2247 (2004)
29. A. Elia, P.M. Lugarà, C. Giancaspro, Opt. Lett. **30**, 998 (2005)